HHS Public Access

Author manuscript

ACS Sens. Author manuscript; available in PMC 2026 March 21.

Published in final edited form as:

ACS Sens. 2025 October 24; 10(10): 7218–7230. doi:10.1021/acssensors.4c03465.

On the design, fabrication, and operation of electrochemical aptamer-based sensors

Yuyang Wu[1], **Kevin W. Plaxco**[1,2]

[1]Department of Chemistry and Biochemistry, University of California Santa Barbara, Santa Barbara, CA 93106, USA

[2]BioEngineering Department, University of California Santa Barbara, Santa Barbara, CA 93106, USA

Abstract

Electrochemical aptamer-based (EAB) sensors are the only high-frequency, real-time molecular measurement approach reported to date that is simultaneously both (1) selective enough to deploy in situ in the body and (2) independent of the chemical reactivity of its target, rendering it generalizable to the measurement of a wide range of analytes. To date, for example, a half dozen research groups have demonstrated the ability of EAB sensors to support few-second to sub-second resolved, multi-hour measurements of drugs and biomarkers in the veins, brains, and solid peripheral tissues of live rats. Motivated by the scientific and clinical applications these real-time, highly-time-resolved in vivo measurements enable, significant literature has explored methods for improving the design, fabrication, and operation of EAB sensors. Here we critically review this literature in an effort to identify what we believe are the most promising of these approaches and which are the areas of EAB sensor design, fabrication, and operation that remain to be profitably explored.

Graphical Abstract

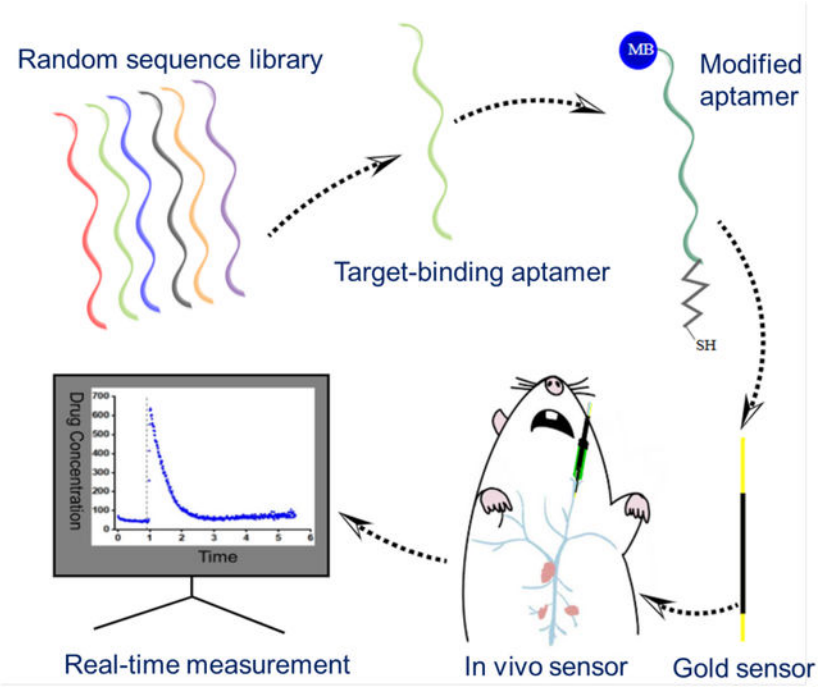

Keywords

Aptamer design; biosensor; deposition; in vivo sensor; redox reporter; self-assembled monolayer; sensor interrogation; stability

The extraordinary versatility, specificity, and affinity with which biomolecules recognize their target ligands have motivated more than 60 years of research into harnessing such receptors into analytical technologies[1]. Despite these efforts, however, the continuous glucose monitor employed in the monitoring and treatment of diabetes[2] the only commercially and clinically successful, single-step device (as opposed to multistep processes, such as ELISAs and lateral flow assays) to emerge from these decades' worth of effort. And because the glucose monitor relies on the ability of enzymes (glucose oxidase or glucose dehydrogenase) to convert its target into electrochemically-detectable product, this approach to molecular monitoring has proven difficult to adapt to any but a handful of other targets[3]. In short, the dream of developing a platform technology able to perform the high-frequency, real-time measurement of almost any arbitrary molecule, irrespective of its chemical reactivity, in situ in the body remains a major aim of the biosensor field[4].

Towards achieving the long-sought goal of generalizable, in vivo molecular measurements, we[5–10] and others[11–14] are developing Electrochemical aptamer-based (EAB) sensors (Fig. 1A–B). Signal generation in this class of sensors occurs when an electrode-bound, redox-reporter-modified aptamer undergoes a binding-induced conformational change, such as binding-induced folding or binding-induced displacement of the redox reporter from the target-binding cleft[15], or when the bound target sterically blocks the reporter from approaching the surface[16]. This causes a change in the rate of electron transfer to and from the reporter, producing in turn an easily measurable electrochemical output when

such sensors are interrogated via any of a number of transfer-rate-sensitive electrochemical techniques. This signal transduction mechanism underlies the two important advantages EAB sensors have over other biosensor architectures. First, because it does not rely on the chemical transformation of the target, EAB sensors can be generalized to the detection of many targets, with existing examples including sensors against a wide range of metabolites[10,17,18], therapeutic drugs[12,17,19], abused drugs[6,20,21], toxins[22], proteins[5,23,24] and hormones[13]. Second, because it mimics the conformation-linked signaling of naturally occurring chemoperception systems, EAB sensors are selective enough to deploy in unprocessed biological fluids and other, equally complex samples, including undiluted saliva[6], foodstuffs[22], urine[24], blood serum[7,8,23], and whole blood[25,26]. Indeed, EAB sensors even support real-time, high-temporal-resolution (to sub-second[27]) molecular monitoring in situ in the living body (Fig. 1C, D)[9,14,19,21,28–30], an ability that, in turn, supports such advances as closed-loop, feed-back controlled drug delivery[9,28,30].

Given the potential clinical and scientific advances that could be enabled by real-time, high-frequency, in vivo molecular measurements, significant effort has gone into optimization of the design, fabrication, and operation of EAB sensors. The community of researchers working on these sensors have shown, for example, that their performance depends upon such design properties as the manner in which the aptamer is modified to produce a binding-induced signal change, the redox reporter used to generate the electrochemical signal, the chemistry of monolayer employed to attach the aptamer to the electrode, and the morphology of the electrode surface. Not surprisingly, EAB sensor performance is also a function of the conditions employed during sensor fabrication and the electrochemical approach used in sensor interrogation. Here we provide a critical review of much of these literatures, describe the optimization steps we employ in our group when creating new EAB sensors, and highlight additional areas of exploration that we believe could further enhance the performance of this potentially transformative measurement technology.

A. The signal transduction mechanism

Produced via an in vitro molecular evolution method (known as systematic evolution of ligands by exponential enrichment: SELEX), aptamers were first described in 1990[31–32] and have since been reported for hundreds of molecular targets[33] (Fig. 2A). Many of these, however, do not undergo any significant conformational change upon target binding (since this is not generally a selection criterion), rendering them unsuitable for use in EAB sensors[10,35]. To overcome this, several approaches have been described by which newly selected aptamers can be systematically re-engineered such that they produce a robust signal change when employed in such sensors.

While some aptamers produce an EAB signal change without any modification following their selection, most do not, thus requiring additional modifications to produce this necessary condition. This involves destabilizing the aptamer's folded, target-binding conformation, either by truncation (Fig. 3A), the insertion of a long, flexible loop (Fig. 3B), or the introduction of a complementary strand (Fig. 3C). This coupling of binding to an unfavorable conformational change produces a tradeoff between affinity and signal gain (the relative change in signal upon target binding). This is because, the more unfavorable the

conformational change, the more aptamers that are poised to change and, thus, the higher the gain. Conversely, however, the more unfavorable the conformational change, the poorer the affinity, since binding is competing with the unfavorable conformational change[36]. For example, the binding affinities of a systematic series of truncations of a vancomycin aptamer range from 0.14 to 52 μM, with the signal gain of the resulting EAB sensors concomitantly increasing from 50% to 150%[37]. Given the confounding relationship between affinity and gain, we typically explore a number of different truncations of each aptamer to identify the sequence that achieves the best trade-off between the two[10]. Because the fabrication of redox-reporter-and-thiol modified aptamers can be expensive, spectroscopic or calorimetric methods, which can be performed using unmodified oligonucleotides, are often used as a rough guide to such truncation[10,38,39]. As a more systematic means of improving the ease of identifying appropriate truncations, however, Alkhamis et al. have used nuclease digestion to identify structure-switching aptamers[40]. Specifically, they identify the minimum length construct that is resistant to exonucleases in the presence of target, finding that these often undergo large conformational changes upon binding, producing in turn high-gain EAB sensors[41].

A second method of introducing a binding-induced conformational change into aptamers is via the introduction of long, unstructured loop, the unfavorable closure entropy of which renders the aptamer unfolded in the absence of target (Fig. 3B). In an early example of this, we inserted an unstructured, 60-base polythymine linker into the middle of a cocaine-binding aptamer[41]. The 175% gain of the resulting sensor is notably higher than the 50% gain of an otherwise equivalent sensor for which binding-induced folding was introduced via truncation, suggesting to us that further exploration of this design approach is in order.

A third method of generating a binding-induced conformational change is to introduce an antisense sequence, such that target binding shifts the aptamer-plus-antisense pair from a helical duplex to the aptamer's target-binding conformation (Fig. 3C), with the above-described trade-off between affinity and gain being tuned by adjusting the hybridization potential of the introduced antisense sequence[35]. In the first example of this, Xiao et al. demonstrated a thrombin-detecting sensor that achieves an impressive, 270% signal gain[5]. In this and other reported examples[35], the antisense strand was attached to the aptamer via a region of complementarity that is not disrupted by binding, likely rendering the architecture reversible. By employing a complementary strand that dissociates entirely upon target binding, however, Zuo et al. produced up to 10-fold gain in an ATP-detecting EAB sensor, albeit at the cost of losing reversibility[42]. And while the strand displacement mechanism does not always produce higher gain than other EAB signal transduction mechanisms[35], given the impressively high gain it may produces, we believe that the approach likewise deserves rather more study than it has seen to date. Particularly given that it is possible to build such constructs from a single, fully-covalent strand[43] (see, by analogy, ref[43]), which would render such sensors more stable.

Finally, we must note that EAB signal generation need not require a binding-induced conformational change in the aptamer itself. Early on, for example, we showed that a thrombin-detecting sensor performs acceptably well under solution conditions in which its target-binding-aptamer is folded in the absence of target[15], suggesting that, because of steric

effects, the binding of this modestly large protein is sufficient to reduce the efficiency with which the redox reporter approaches the electrode surface. The gain of this sensor, however, is only half that seen under solution conditions in which the aptamer undergoes binding-induced folding. More recently, Dauphin-Ducharme et al. have argued that signal generation in some aptamers arises due to target-induced displacement of the redox reporter from the target-binding-cleft[16]. We believe that we have likewise seen such behavior in a phenylalanine-detecting sensor[10]. We note, however, that, unlike conformation-linked mechanisms, which can be introduced into any aptamer, it is unclear how this signal transduction mechanism can be rationally introduced into new aptamers, thus raising questions regarding its generality.

B. Thiol and reporter placement

Most of the reported EAB sensors employ a thiol group on their 3' terminus to anchor the aptamer to the electrode surface, placing the redox reporter on the 5′ terminus. Having reversed this for several EAB sensors, however, we found that gain is a strong function of the attachment site location[44]. Specifically, we tested three different aptamers, and found that the gain of all of the resulting sensors is higher when their aptamer is anchored via its 5′ terminus. Perhaps not coincidentally, the aptamers employed in this study are all thought to bring their termini together to form a double helix, and double-stranded DNAs attached to a surface via a 5′ anchor are said to adopt a more vertical orientation than those anchored via their 3′ end[45]. Nevertheless, given the broad structural diversity of aptamers, we suspect that some aptamers may behave in the inverse manner. Given this and given that it is relatively easy to test the two orientations empirically, we believe that such characterization can be profitably added to the EAB sensor design workflow.

The significant impact that switching the termini that are modified with the anchoring thiol and the redox reporter has on gain leads us to suspect that placing the redox reporter or the anchoring thiol at positions within the chain could also enhance performance. To date, however, exploration of this remains limited. Despite the fact that the requisite internal-thiols are commercially available[43], for example, we have not seen any exploration of EAB sensors employing internal anchoring site. And we have seen only 3 examples in which internal redox reporter sites have been employed, likewise despite their ready commercial availability. In the first of these, Mayer et al. placed redox reporter at the distal end, on an internal base, and on a base near the electrode-attachment site of a TNF-α aptamer, finding found that the construct with the distally-situated reporter produced the highest gain[46]. In contrast, in the second Gerasimov et al. found that the gain of an insulin-detecting sensor with an internally placed reporter is 1.5-fold greater than that of an equivalent sensor employing a redox reporter on the distal terminus. Finally, Bakhshandeh et al. employed internal methylene blue reporters in a lactate sensor and a glucose sensor, though they did not report any comparison with the performance of the equivalent, terminally modified sensors[47]. Reviewing this still-sparse literature, our suspicion is that exploration of alternative anchor and reporter placements may prove fruitful.

C. The redox reporter

In an early effort to identify redox reporters suitable for use in EAB-type sensors (i.e., sensors that, like EAB sensors, are comprised of a redox-reporter-modified DNA attached via a thiol-on-gold SAM to a gold electrode), we characterized E-DNA sensors employing a range of redox moieties that are commercially available in forms easily conjugatable to DNA[48]. To our surprise at the time, the performance of the resulting sensors varied enormously. Many, for example, failed to produce clear, single oxidation and reduction peaks and some proved difficult to conjugate to DNA or exhibited unacceptably large changes in redox potential upon conjugation. And only the sensor employing methylene blue exhibited good stability against repeated electrochemical interrogations. Specifically, while methylene blue lost only 2% of its initial current after 100 square-wave voltametric scans, the signaling current of sensors employing anthraquinone, Nile blue, or 5′-linked ferrocene fell by 50% under these conditions, and that of sensors fabricated using 3′-linked ferrocene, ferrocene-C5, or penta-methyl ferrocene fell even more dramatically. In short, the stability of sensors fabricated using methylene blue stands out among all of the reporters we have investigated. Given that the redox potential of methylene blue lies almost exactly in the middle of the potential window over which alkane-thiols-on-gold are stable[49], we believe this is due to electrochemical desorption of the monolayer at the redox potentials of the other reporters we have characterized. With this in mind, the recently described ATTO 700 reporter, the redox potential of which lies near the center of the stability window for these monolayers, may be of interest[58].

Despite its near universal application to date, and its significant positive attributes, methylene blue as an EAB reporter is not without limitations. First, because it is a 2-electron, 1-proton redox couple, the reporting properties of methylene blue are pH dependent. This harms sensor calibration in pH-variable sample matrices, such as sweat or saliva. Thus motivated, Li et al. have explored a π-extended tetrathiafulvalene called exTTF as a reporter[50]. This pro-aromatic electron donor undergoes a single, two-electron oxidation process that, because it does not involve proton transfer, is insensitive to pH. And, conveniently, its redox potential is also reasonably near the middle of the potential range over which thiol-on-gold SAMs are stable. Following this, Pellitero et al. have described a similarly pH-insensitive Os(II/III) complex that, in head-to-head comparisons, exhibits better stability than methylene blue[51]. Specifically, when serially interrogated in a simple buffer every 8 s for 48 h, a sensor employing the osmium complex lost only 25% signal, versus the 60% signal loss seen for the equivalent, methylene blue-functionalized sensor. A second limitation of methylene blue as a reporter is its rather sluggish intrinsic electron transfer rate, which limits the rate at which EAB sensors can be interrogated and, as discussed below, likely also limits the thickness (and thus stability) of the self-assembled monolayers they can employ. In this light, the more rapid transfer rate of the osmium complex and of the above-mentioned ATTO-700 reporter may also prove of value.

D. Alternative monolayers

Almost all of the EAB sensors reported to date have attached their aptamer to the interrogating electrode using an alkane-thiol-on-gold self-assembled monolayer (SAM),

with most of these employing a hydroxyl-terminated, 6-carbon thiol. Increasing the number of thiols[52] or the monolayer thickness (by extending the length of the alkane-thiol)[53], however, is known to improve monolayer stability. Thus motivated, Watkins et al. compared the performance of EAB sensors fabricated using either 6-mercapto-1-hexanol or 8-mercapto-1-octanol (using a methylene blue reporter), finding that the latter produce similar gain, but are more stable when challenged for 7 days in 37 °C a simple buffer[54]. In our experience, however, going to still thicker monolayers can lead to unacceptably slow electron transfer rates (unpublished results).

While it is clear that EAB sensor performance is also sensitive to the chemistry of the monolayer surface, this parameter has seen relatively little exploration. In one example, however, a phosphatidylcholine-terminated monolayer, which mimics the head-groups seen in the cell membrane, reduces the drift seen in 37°C whole blood by an order of magnitude[55]. Indeed, drift is reduced so much that, when the resulting sensors achieved fairly good (to within a few percent) return to baseline after more than 6 h in situ in the veins of live animals without the use of drift-correction algorithms (see below). More recently, the Arroyo-Currás group reported that a methyl-terminated monolayer (i.e., presenting a hydrophobic surface) enhances EAB sensor stability in undiluted serum held at room temperature[52]. Specifically, while the signal of sensors employing a methyl-terminated monolayer remains virtually unchanged after 2 days of continuous interrogation in 37 °C whole blood, that of a sensor employing the traditional, hydroxy-terminated monolayer lost almost all of its signal. This methyl-terminated surface, however, reduced overall signal gain, and its effect on aptamer affinity varies with from sensor to sensor. For example, the affinity of a vancomycin-detecting sensor does not change much (from 151 ± 9 μM for the hydroxyl-terminated surface to 187 ± 18 μM for the methyl), worsens for a doxorubicin sensor (from 1.63 ± 0.05 μM to 15.8 ± 0.8 μM), and improves for a tobramycin sensor (from 154 ± 2 μM to 9.8 ± 0.3 μM).

Recently, Kesler et al. report that the use of a homogeneously carboxylate-terminated monolayer simultaneously increases both the gain of a doxorubicin-detecting sensor and its affinity for its target[56]. We have found, however, that such monolayers can prove unstable, presumably due to unfavorable charge-charge interactions between the carboxylic acid head groups[57]. Thus motivated, we have explored mix monolayers comprised of 6-carbon hydroxyl terminated thiols, and either 6- or 8-carbon, carboxylate-terminated monolayers. Doing so, we found that the addition of order 50% carboxylate head groups increased the gain of all 3 of the sensors we characterized without significantly reducing their stability. These promising results aside, we encourage researchers to explore this “space” further, as we suspect that, given the enormous range of possible surface chemistries accessible, the optimal surface has likely not yet been identified.

E. Alternative electrode materials and attachment chemistries

Given the convenience and reasonable performance of the chemistry, almost most every EAB sensor described to date has been fabricated using alkane-thiol-on-gold monolayers. This chemistry, however, is not without a potentially important limitation. Specifically, the potential window over which such monolayers are stable (e.g., >80% of the peak current

remains after 1500 scans) only spans of order 0.5 V (from about +0.05 V to about −0.40 V versus Ag/AgCl[49]), which limits, for example, the extent to which we can "multiplex" such sensors via the use of multiple reporters each reporting at distinct redox potentials[48,58]. In response, we are aware of a number of groups (ourselves included) who have tried but failed to adapt EAB sensors to carbon electrodes (unpublished observations). And while Shaver et al. successfully used amide-formation to site-specifically attach a redox-reporter-modified aptamer onto conductive polymers, the resulting sensor was unstable and quite sensitive to nonspecific interferents[59]. Indeed, the only successful example we know of in which EAB sensors were fabricated using chemistry other than alkane-thiols on gold was a recent study in which an alkyne-gold bond was employed[60]. The results of this chemistry were mixed, however: while the stability of sensors employing this chemistry appears to be slightly better than that of sensors fabricated using alkane-thiols-on-gold, and the gain of a tobramycin-detecting sensor doubled on the alkyne-on-gold surface (50% versus 25%), the gain of an ATP-detecting sensor collapsed when this new chemistry was employed. We note, too, that it is unclear whether the potential window over which this alkyne chemistry is stable against EAB sensor interrogation is any broader than that of alkane-thiols-on-gold.

F. Protection from electrode fouling and aptamer degradation

EAB sensors exhibit significant time-dependent signal loss when deployed in bodily fluids, particularly at physiological temperatures. This is caused by both fouling and the enzymatic degradation of the target-recognizing aptamer, with the former seeming to dominate in body-temperature whole blood in vitro[49] and the latter in blood in vivo[61]. Fortunately, there are a number of electrochemical methods by which this drift can be corrected or circumvented (described in detail in section III), thus ensuring that good measurement accuracy is retained even in the presence of drift. Nevertheless, the associated loss in peak current reduces signal-to-noise ratios, ultimately limiting the duration of in vivo measurements. This has motivated a number of groups to study methods of reducing this drift.

To date, a handful of papers have appeared in which hydrogel coatings have been used to reduce EAB sensor drift, presumably by reducing the rate with which nucleases and other blood components reach the electrode surface[54,62,63,64]. In the most detailed of these, the Li group employed an agarose gel to significantly reduce the drift seen when the sensor is deployed both in vitro in undiluted whole blood at room temperature and in vivo in the veins (Fig. 4A), bladder, and solid tissues of live rats[64]. Indeed, the signal drift was reduced so much that the gel-protected in vivo sensors achieve clinically relevant accuracy without employing drift correction algorithms. The gel-protected sensors also exhibit good biocompatibility: intravenously or intramuscularly implanted sensors produce no detectable impact on blood counts or histology (this said, though, we note that the biocompatibility of unprotected sensors has not been reported and could be similarly good). Of note, the use of the hydrogel did not significantly reduce the sensor's equilibration time against a low-molecular-weight target.

More recently, the Heikenfield group has described the use of a zwitterionic polybetaine hydrogel to protect EAB sensors against fouling[54]. This improved the drift properties of sensors employing both mercaptohexanol and mercaptooctanol monolayers in 37 °C bovine

serum in vitro. Oddly, however, this protective layer reduced the gain of sensors using the latter monolayer while leaving the gain of sensors employing the latter monolayer unchanged. Finally, Santos-Cancel et al. report that hydrogels containing entrapped ribonuclease inhibitors improve the stability of an EAB sensor employing an RNA-aptamer when it is challenged in nuclease-containing bodily fluids, including serum and whole blood[63]. Specifically, the authors coated an EAB sensor employing an RNA aptamer against the aminoglycoside antibiotics with a collagen I hydrogel pretreated with ribonuclease inhibitors, finding that the resulting sensor maintained good performance in undiluted serum for at least 6 h. The signal of an unprotected sensor, in contrast, fell by 98% under the same conditions. In general, we view such hydrogels as a promising approach to reducing the drift of in vivo EAB sensors, though we must note that such protection is likely incompatible with sensors against proteins or other larger analytes due to the slow diffusion of such targets through the hydrogel.

As an alternative to preventing the approach of nucleases to the sensor surface, we have recently explored the feasibility of rendering the aptamer itself nuclease resistant[61]. We did so by fabricating the aptamer from xenonucleic acids (XNA), synthetic nucleic acid analogues employing a polymer backbone that differs from either ribose or deoxyribose[65]. Many of the altered backbones used in XNAs are resistant to nuclease digestion, suggesting their use might reduce the signal drift seen when EAB sensors are deployed in vivo. Thus motivated, we fabricated a tobramycin-detecting EAB sensor employing a 2'-methoxy-RNA aptamer[61]. When deployed in the jugular of a live rat, this sensor exhibited only a few percent loss in signal over the course of several hours (Fig. 4C). In contrast, under the same conditions the signal from a sensor employing the equivalent DNA aptamer fell by nearly half. This, obviously, is only a single example, but given the increasing ease with which XNA aptamers can be selected[66–68], we believe that they will prove a valuable addition to the EAB platform.

II. Sensor fabrication

Two elements of the EAB sensor fabrication process –increasing the microscopic surface area of the gold (i.e., the atomic-scale surface area) and regulating conditions under which the aptamer-decorated monolayer is formed– have proven important elements in optimizing EAB sensor performance.

A. Electrode morphology

The signaling current of an EAB sensor, which is proportional to the number of redox-reporter-modified aptamers on its surface, can be increased by using larger electrodes. For size-limited applications, however, such as placements in vivo, this approach to improving signal-to-noise ratios is often sub-optimal. Given this, we have instead focused on improving EAB signaling currents by increasing the microscopic surface areas of our electrodes. In our first approach to this end, we used "electroroughening" via chronoamperometric pulsing to increase the microscopic surface area of gold-wire electrodes, leading to ~2-fold increases in signal-to-noise ratios for sensors deployed in the rat jugular[69] (Fig. 5). Following this, Li et al. demonstrated the use of shrink-wrinkled gold-coating polyolefin film to increase the

microscopic surface area of gold electrodes up to 10-fold[70]. This approach, however, has not yet been applied in vivo. Finally, in 2021, we applied an electrochemical de-alloying process to create nanoporous gold, thus increasing the microscopic surface area up to 100-fold and EAB signaling current by up to 30-fold[71]. This was sufficient to enable miniaturization of a 75 μm-diameter and 0.5 mm long EAB sensor that retained excellent signal-to-noise ratios when deployed in the rat jugular.

B. Optimizing aptamer deposition

The density with which the target-recognizing aptamers are packed onto the sensor surface strongly affects the gain of EAB sensors, with the optimal packing density varying from aptamer to aptamer. For example, optimal packing density increases the signal gain of a cocaine-detecting sensor more than 3-fold relative to the poorest performing packing density[72] (Fig. 6A). Given its importance, we regard the optimization of aptamer packing density (which we perform by varying the aptamer concentration employed during deposition) a high priority in our sensor fabrication workflow.

Although not yet well explored, we suspect that the solution conditions under which the aptamers are immobilized on the electrode surface also affect sensor performance. Across multiple sensors, for example, Liu et al. have found that performing aptamer deposition at pH 6.0 yields noticeably lower gain than fabrication at pH 7.4[74]. And for 2 sensors they found that fabrication at lower ionic strength improves gain by 1.2- and 1.5-fold. Surprisingly to us, the latter occurs despite the higher ionic strength having little effect on packing density. To the best of our knowledge, however, the effects of pH and ionic strength on EAB sensor fabrication have not yet been described by others.

The formation of alkane-thiol-on-gold monolayers in general is sensitive to temperature, and thus altering the deposition temperature could impact sensor performance. Liu et al. report, for example, that freezing facilitates the assembly of high-density DNA-modified monolayers on gold nanoparticles[75], which they attribute to the freezing-induced stretching and alignment of the DNA. Applying this observation to the fabrication of a doxorubicin sensor (by dropping aptamer solution on a freshly cleaned gold surface and then freezing the surface for 15 min at −20 °C), they report that it improves stability. For example, after 4 h of interrogation in fetal bovine serum, the signal of cold-fabricated sensors fell by only 25%, versus the 45% loss seen for the equivalent sensor fabricated at room temperature[76]. The authors also report improved sensor-to-sensor reproducibility (3% versus 14% relative standard deviation of the peak current) and significantly enhanced target affinity. To the best of our knowledge, however, this perhaps surprising result has not yet been repeated for other sensors or by other groups.

EAB sensors are most often prepared via “sequential” deposition, in which the electrode is incubated in a solution of thiol-modified aptamer for 1 h and then “backfilled” via an overnight incubation in dilute mercaptohexanol. There have also been reports, however, of EAB sensors fabricated via a “codeposition” method employing a single-step incubation in a mixture of mercaptohexanol and thiol-modified aptamer[52,77,78,79]. Recently we have compared the performance of sensors fabricated using these two approaches, finding that the latter typically improves gain by 1.2 to 1.7-fold[73] (Fig. 6B). Moreover, as a single-step

process, codeposition can be completed in 1 h, rendering it somewhat more convenient than the traditional, overnight sequential method. This said, this approach does not work for all aptamers. For example, it leaves the gain of a phenylalanine-detecting sensor unchanged. Given how easy it is to explore this alternative fabrication approach, however, we now include characterization of this when fabricating a new type of EAB sensor.

Finally, it appears that EAB sensor gain is significantly improved by performing the aptamer deposition in the presence of the target molecule (Fig. 6B). Specifically, the Xiao group reported that target-assisted deposition improved the signal gain of a cocaine-detecting sensor by 1.2-fold, and sensors against methylenedioxypyrovalerone and adenosine by 1.5-fold[74]. This presumably occurs because target binding folds the aptamer prior to deposition, thus reducing the number of aptamers that bind to the surface in a manner that precludes their binding-induced folding. Building on their work, we have found that target-assisted deposition similarly improves the gains of vancomycin- and tryptophan- detecting sensors and does so in a manner that is additive with the gains associated with the co-deposition method described above[73]. Curiously, neither target-assisted deposition nor co-deposition had any significant effect on the gain of a phenylalanine-detecting sensor. Spectroscopic studies suggest, however, that the aptamer employed in the latter sensor remains folded even in the absence of target, thus perhaps explaining why both deposition in the presence of target and co-deposition failed to increase this sensor's gain. We now employ this target-assisted method in the fabrication of all of our sensors, save for those few (e.g., methotrexate; unpublished) for which the binding of target to the bare gold electrode interferes with monolayer formation.

III. Sensor operation

A number of electrochemical approaches have been used to transduce the binding-induced conformational change underlying EAB sensor operation into an easily measurable output, including both voltametric (cyclic, square wave, alternating current, differential pulse) and non-voltametric (chronoamperometry, intermittent pulse amperometry, electrochemical impedance spectroscopy) methods, all of which are sensitive to the binding-induce change in electron transfer rate that underlies signal transduction in the EAB platform. But not all of these approaches are equally well suited to perform EAB sensor interrogation.

A. Voltametric interrogation

The first reported DNA-based electrochemical sensors employed cyclic voltammetry in their interrogation[80]. This approach, however, is less sensitive to transfer rate than many other voltametric methods, it has largely fallen out of favor, being replaced first by alternating current voltammetry[6,81] and differential pulse voltammetry[11] before these were all largely supplanted by square wave voltammetry[82]. We have recently compared the performance of the latter 3 methods, finding that square wave voltammetry generally produces the largest signal gain and the best signal-to-noise ratios[83]. Consistent with this, we use square wave voltammetry for the large majority of our in vivo EAB sensor studies. Before doing so, we always optimize the square-wave frequency[72] and amplitude[84] employed.

In addition to the generally higher gain and improved signal-to-noise ratios it produces, square wave voltammetry also delivers another important advantage: it provides an accurate means of correcting the drift seen when unprotected EAB sensors are deployed in the body. Specifically, gain is such a strong function of square-wave frequency that most sensors exhibit “signal-on” behavior (i.e., target binding increases current) at some frequencies and signal-off behavior at others. By finding pairs of signal-on and signal-off frequencies that drift in concert, we can remove the drift by using an approach termed “kinetic differential measurements”[29,85], where the KDM signal is generally given by:

$$KDM = \frac{s_1 - s_2}{0.5(s_1 + s_2)}$$

Eq. 1

where s_1 and s_2 represent the normalized signal recorded at “signal-on” and “signal-off” frequencies, respectively. Using this approach, we see good sensor accuracy even under such high-drift conditions as days-long measurements in undiluted, whole blood held in vitro at 37°C[61] (Fig. 7A). A limitation of traditional kinetic differential measurements, however, is that it employs relative signal change. That is, the signals observed relative to the signals observed in the absence of target, with the latter being measured for each individual sensor prior to use. Recently, however, we have described a “ratiometric” kinetic differential measurement drift correction approach that avoids the need to perform this zero-target calibration measurement for each, individual sensor.[86] To do so it employs a modified version of KDM:

$$rKDM = \frac{Ri_1 - i_2}{0.5(Ri_1 + i_2)}$$

Eq. 2

Here R is the ratio of the currents measured in the absence of target at the signal-on and signal-off frequencies for all sensors in the fabrication batch, and i_1 and i_2 are the peak currents measured at the two square-wave frequencies employed. That is, this approach uses calibration parameters derived from a subset of the sensors in a batch to calibrate all of the sensors in that batch, with little loss in accuracy.

B. Non-voltametric interrogation

Non-voltametric methods have also been used to interrogate EAB sensors, some of which may provide advantages over voltammetry. The first reported of these, chronoamperometry, measures electron transfer kinetics directly by determining the lifetimes of current transients generated in response to stepping the potential to values at which the redox reporter is fully oxidized or reduced. This produces an exponential current response, the lifetime of which is monotonically related to target concentration[27]. The length of this transient is rather short and thus, using chronoamperometry to measure plasma tobramycin concentrations in the rat jugular, we have achieved a time resolution of 300 ms (Fig. 7C). And because the lifetime of an exponential decay is independent of its amplitude (i.e., independent of the number of reporter-modified-aptamers on the electrode), chronoamperometric interrogation is both

calibration-free and drift resistant. This said, to date the approach has seen relatively little investigation as a means of interrogating EAB sensors; we suspect that this merits more detailed exploration.

The use of intermittent pulse amperometry (IPA) also supports high-frequency EAB sensor interrogation. That is, by alternating between a negative overpotential to reduce the methylene blue reporter and a potential that re-oxidizes it, Santos-Cancel demonstrate that absolute current values at a defined times after the application of the pulse are quantitatively related to the concentration of target analyte[87]. Using this method, the authors were able to interrogate an EAB sensor in less than 5 ms per measurement. This said, we suspect that, under these conditions, the equilibration time of the sensor likely becomes limiting, and thus the sensor's true temporal resolution is probably rather poorer than this impressive, 5 ms interrogation time. We note, too, that this approach has not yet been demonstrated in in vivo applications.

Electrochemical impedance spectroscopy (EIS) has also proven a potentially powerful means of EAB sensor interrogation. EIS measures changes in interfacial surface properties (i.e., charge transfer and electric double layer formation) by applying a sinusoidally oscillating, AC potential wave and measuring the resulting sinusoidal current response. In our first attempt to exploit this for EAB sensor interrogation[88] we used changes in the phase of the current response to monitor target binding, thus achieving sub-second temporal resolution (from 6 to 350 ms, depending on the required AC frequency) and multi-hour stability for measurements performed in vitro in undiluted, whole blood held at 37 °C. Building on this, we next applied fast Fourier transform electrochemical impedance spectroscopy to the problem of interrogating EAB sensors[36]. This method measures the electron transfer rate associated with EAB sensors and thereby determines the concentration of their molecular targets with time resolution of 2 s or better. Since this approach uses electron transfer rate directly to monitor target concentration, rather than absolute current, it is independent of the number of aptamers on the surface, rendering it calibration-free. It has also proven resistant to the drift seen in body temperature biological fluids. Using this to interrogate vancomycin and phenylalanine sensors, for example, we have performed real-time, 1.8 s resolved, calibration-free molecular measurements in situ in the veins of live rats (Fig. 7D). As is true with chronoamperometry, however, we have not yet conducted head-to-head comparison of this approach with square wave voltammetry, and thus, other than time resolution (for which chronoamperometry is better than EIS, which is better than voltammetry), the relative merits of these approaches remain undefined.

Conclusions.

In the nearly 20 years since the first was reported, EAB sensors have been the focus of hundreds of studies by dozens of research groups. Reviewing the data through the prism of our own experience, here we have described the various design, fabrication, and operational parameters that we currently believe are important -or has the potential to be important- elements in achieving the highest possible EAB sensor performance. Our goal in doing so is to facilitate the application of EAB sensors. And while we have focused primarily on in vivo measurements in this work (as that is our primary area of interest), we close

by noting that, in addition to application to pharmacokinetics performed in live animals, clinical applications focused on ex vivo samples (urine, serum, sweat, saliva, etc.) are likely a valuable potential application for those targets for which daily monitoring, rather than real-time, seconds-resolved data, capture the majority of the clinical value. We note, too, that there are many other potentially valuable applications of the technology, such as performing feed-back control in fermentation and cell culture, and monitoring the response of organoids and organ-on-a-chip to drugs for drug screening and evaluation. We look forward to seeing further developments in these exciting areas.

Vocabulary

Drift
The loss in raw signal seen when EAB sensors are interrogated in vivo using voltametric methods.

Electrochemical, aptamer-based (EAB) sensor
A platform molecular sensing technology that utilizes a binding-induced conformational change in an electrode-bound, redox-reporter-modified aptamer to produce an easily measurable electrochemical signal.

Gain
The relative change in signal seen between the absence of target and saturating (or some other high, well-defined) target concentration.

Kinetic differential measurements (KDM)
An electrochemical that method that removes the drift seen when EAB sensors are deployed in vivo by taking the difference between the relative signals seen at “signal-on” (i.e., target binding increases current) and “signal-off” square wave voltammetry frequencies.

Self-assembled monolayer (SAM)
Single-molecule-thick molecular assemblies spontaneously formed on surfaces. The work described here employs those formed by alkane thiols on gold surfaces.

Sensor interrogation
Measurement of target by applying an electrochemical method, such as voltammetry, chronoamperometry, or electrochemical impedance spectroscopy, to an electrochemical sensor.

Stability
The ability of an EAB sensor to retain consistent signaling properties after prolonged, repeated interrogation.

Reference:

1. Bhalla N, Jolly P, Formisano N, and Estrela P, “Introduction to biosensors.” Essays in biochemistry, 2016, 60, 1–8. [PubMed: 27365030]
2. Yoo EH, Lee SY, “Glucose biosensors: an overview of use in clinical practice.” Sensors., 2010, 10, 4558–4576. [PubMed: 22399892]

3. Wang S, Liu Y, Zhu A and Tian Y “In vivo electrochemical biosensors: recent advances in molecular design, electrode materials, and electrochemical devices”, Anal. Chem, 2023, 95, 388–406. [PubMed: 36625112]
4. Rong G, Corrie SR, and Clark HA, “In vivo biosensing: Progress and perspectives.” ACS sensors, 2017, 2, 327–338. [PubMed: 28723197]
5. Xiao Y, Lubin AA, Heeger AJ, and Plaxco KW “Label-free electronic detection of thrombin in blood serum by using an aptamer-based sensor.” Angewandte Chemie, 2005, 44, 5456–5459. [PubMed: 16044476]
6. Baker BR, Lai RY, Wood MS, Doctor EH, Heeger AJ, and Plaxco KW, “An electronic aptamer-based small-molecule sensor for the rapid, label-free detection of cocaine in adulterated samples and biological fluids.” JACS, 2006, 128, 3138–3139.
7. Lai RY, Plaxco KW, and Heeger AJ, “Aptamer-based electrochemical detection of picomolar platelet-derived growth factor directly in blood serum.” Anal. Chem, 2007, 79, 229–233. [PubMed: 17194144]
8. Swensen JS, Xiao Y, Ferguson BS, Lubin AA, Lai RY, Heeger AJ, Plaxco KW, and Soh HT, “Continuous, real-time monitoring of cocaine in undiluted blood serum via a microfluidic, electrochemical aptamer-based sensor.” JACS, 2009, 131, 4262–4266.
9. Dauphin-Ducharme P, Yang K, Arroyo-Currás N, Ploense KL, Zhang Y, Gerson J, Kurnik M, Kippin TE, Stojanovic MN, and Plaxco KW, “Electrochemical aptamer-based sensors for improved therapeutic drug monitoring and high-precision, feedback-controlled drug delivery.” ACS Sensors, 2019, 4, 2832–2837 [PubMed: 31556293]
10. Wu Y, Ranallo S, Del Grosso E, Chamoro-Garcia A, Ennis HL, Milosavić N, Yang K, Kippin T, Ricci F, Stojanovic M, and Plaxco KW “Using spectroscopy to guide the adaptation of aptamers into electrochemical aptamer-based sensors.”, Bioconj. Chem, 2023, 34, 124–132
11. Radi AE, Acero Sánchez JL, Baldrich E, and O’Sullivan CK, “Reagentless, reusable, ultrasensitive electrochemical molecular beacon aptasensor.” JACS, 2006, 128, 117–124.
12. Schoukroun-Barnes LR, Wagan S, and White RJ, “Enhancing the analytical performance of electrochemical RNA aptamer-based sensors for sensitive detection of aminoglycoside antibiotics.” Anal. Chem,2014, 86, 1131–1137. [PubMed: 24377296]
13. Singh NK, Chung S, Sveiven M, and Hall DA, “Cortisol detection in undiluted human serum using a sensitive electrochemical structure-switching aptamer over an antifouling nanocomposite layer.” ACS *omega*, 2021, 6, 27888–27897.
14. Lin S, Cheng X, Zhu J, Wang B, Jelinek D, Zhao Y, Wu TY, Horrillo A, Tan J, Yeung J, Yan W, Forman S, Coller HA, Milla C, and Emaminejad S, “Wearable microneedle-based electrochemical aptamer biosensing for precision dosing of drugs with narrow therapeutic windows.” Sci. Adv, 2022, 8, eabq4539
15. Dauphin-Ducharme P, Churcher ZR, Shoara AA, Rahbarimehr E, Slavkovic S, Fontaine N, Boisvert O and Johnson PE, “Redox reporter - ligand competition to support signaling in the cocaine-binding electrochemical aptamer-based biosensor.” Chemistry., 2023, 29, e202300618. [PubMed: 36988081]
16. Xiao Y, Uzawa T, White RJ, DeMartini D and Plaxco KW, “On the signaling of electrochemical, aptamer-based sensors: collision- and folding-based mechanisms.” Electroanalysis, 2009, 21, 1267–1271 [PubMed: 20436787]
17. Idili A, Gerson J, Parolo C, Kippin T, and Plaxco KW, “An electrochemical aptamer-based sensor for the rapid and convenient measurement of L-tryptophan.” Anal. Bioanal Chem, 2019, 411, 4629–4635. [PubMed: 30796485]
18. Bakhshandeh F, Zheng H, Barra NG, Sadeghzadeh S, Ausri I, Sen P, Keyvani F, Rahman F, Quadrilatero J, Liu J, Schertzer JD, Soleymani L, and Poudineh M, “Wearable aptalyzer integrates microneedle and electrochemical sensing for in vivo monitoring of glucose and lactate in live animals.” Adv. Mater, 2024, e2313743. [PubMed: 38752744]
19. Chamorro-Garcia A, Gerson J, Flattebo C, Fetter L, Downs AM, Emmons N, Ennis HL, Milosavic N, Yang K, Stojanovic M, Ricci F, Kippin TE, and Plaxco KW, “Real-time, seconds-resolved measurements of plasma methotrexate in situ in the living body.” ACS Sensors, 2023, 8, 150–157 [PubMed: 36534756]

20. Canoura J, Liu Y, Alkhamis O, and Xiao Y, "Aptamer-based fentanyl detection in biological fluids." Anal. Chem, 2023, 95, 18258–18267. [PubMed: 38033203]
21. Alkhamis O, Canoura J, Wu Y, Emmons NA, Wang Y, Honeywell KM, Plaxco KW, Kippin TE, and Xiao Y, "High-affinity aptamers for in vitro and in vivo cocaine sensing." JACS, 2024, 146, 3230–3240
22. Li H, Somerson J, Xia F, and Plaxco KW, "Electrochemical DNA-based sensors for molecular quality control: Continuous, real-time melamine detection in flowing whole milk." Anal. Chem, 2018, 90, 10641–10645. [PubMed: 30141321]
23. Parolo C, Greenwood AS, Ogden NE, Kang D, Hawes C, Ortega G, Arroyo-Currás N, and Plaxco KW "E-DNA scaffold sensors and the reagentless, single-step, measurement of HIV-diagnostic antibodies in human serum." Microsyst Nanoeng, 2020, 6, 13. [PubMed: 34567628]
24. Parolo C, Idili A, Ortega G, Csordas A, Hsu A, Arroyo-Currás N, Yang Q, Ferguson BS, Wang J, and Plaxco KW, "Real-time monitoring of a protein biomarker." ACS sensors, 2020, 5, 1877–1881. [PubMed: 32619092]
25. Li H, Dauphin-Ducharme P, Ortega G, and Plaxco KW, "Calibration-Free Electrochemical biosensors supporting accurate molecular measurements directly in undiluted whole blood." JACS, 2017, 139, 11207–11213.
26. Downs AM, Gerson J, Leung KK, Honeywell KM, Kippin T, and Plaxco KW, "Improved calibration of electrochemical aptamer-based sensors." Sci. Rep, 2022, 12, 5535. [PubMed: 35365672]
27. Arroyo-Currás N, Dauphin-Ducharme P, Ortega G, Ploense KL, Kippin TE, and Plaxco KW "Subsecond-resolved molecular measurements in the living body using chronoamperometrically interrogated aptamer-based sensors." ACS Sensors, 2018, 3, 360–366. [PubMed: 29124939]
28. Arroyo-Currás N, Ortega G, Copp DA, Ploense KL, Plaxco ZA, Kippin TE, Hespanha JP, and Plaxco KW "High-precision control of plasma drug levels using feedback-controlled dosing." ACS pharmacology and translational science, 2018, 1, 110–118 [PubMed: 32219207]
29. Arroyo-Currás N, Somerson J, Vieira P, Ploense K, Kippin TE, and Plaxco KW, "Real-time measurement of small molecules in awake, ambulatory animals." Proc. Natl. Acad. Sci, 2016, 114, 645–650
30. Gerson J, Erdal MK, McDonough MH, Ploense KL, Dauphin-Ducharme P, Honeywell K, Leung K, Arroyo-Currás N, Gibson J, Meiring W, Hespanha J, Plaxco KW and Kippin TE, "High-precision monitoring of and feedback control over drug concentrations in the brains of freely-moving rats." Sci. Adv, 2023, 9, eadg3254
31. Tuerk C, and Gold L, "Systematic evolution of ligands by exponential enrichment: RNA ligands to bacteriophage T4 DNA polymerase." Science, 1990, 249, 505–510 [PubMed: 2200121]
32. Ellington AD, and Szostak JW, "In vitro selection of RNA molecules that bind specific ligands." Nature, 1990, 346, 818–822. [PubMed: 1697402]
33. Plach M, and Schubert T, "Biophysical characterization of aptamer-target interactions." Adv Biochem Eng Biotechnol, 2020, 174, 1–15. [PubMed: 31375847]
34. Roehrich B, Leung KK, Gerson J, Kippin TE, Plaxco KW, and Sepunaru L "Calibration-free, seconds-resolved in vivo molecular measurements using Fourier-transform impedance spectroscopy interrogation of electrochemical aptamer sensors." ACS Sensors, 2023, 8, 3051–3059. [PubMed: 37584531]
35. White RJ, Rowe AA, and Plaxco KW, "Re-engineering aptamers to support reagentless, self-reporting electrochemical sensors." The Analyst, 2010, 135, 589–594. [PubMed: 20174715]
36. Kang D, Vallée-Bélisle A, Porchetta A, Plaxco KW, and Ricci F "Re-engineering electrochemical biosensors to narrow or extend their useful dynamic range." Angewandte Chemie, 2012, 51, 6717–6721. [PubMed: 22674785]
37. Shaver A, Mahlum JD, Scida K, Johnston ML, Aller Pellitero M, Wu Y, Carr GV, and Arroyo-Currás N "Optimization of vancomycin aptamer sequence length increases the sensitivity of electrochemical, aptamer-based sensors in vivo." ACS sensors, 2022, 7, 3895–3905. [PubMed: 36417705]

38. Lin PH, Chen RH, Lee CH, Chang Y, Chen CS, and Chen WY “Studies of the binding mechanism between aptamers and thrombin by circular dichroism, surface plasmon resonance and isothermal titration calorimetry.” Colloids Surf B Biointerfaces, 2011, 88, 552–558. [PubMed: 21885262]
39. Nakatsuka N, Yang KA, Abendroth JM, Cheung KM, Xu X, Yang H, Zhao C, Zhu B, Rim YS, Yang Y, Weiss PS, Stojanović MN, and Andrews AM “Aptamer-field-effect transistors overcome Debye length limitations for small-molecule sensing.” Science, 2018, 362, 319–324. [PubMed: 30190311]
40. Alkhamis O, Canoura J, Ly PT, and Xiao Y, “Using exonucleases for aptamer characterization, engineering, and sensing.” Acc Chem Res, 2023, 56, 1731–1743. [PubMed: 37314701]
41. White RJ, and Plaxco KW “Engineering new aptamer geometries for electrochemical aptamer-based sensors.” Proc. Natl. Acad. Sci, 2009, 7321, 732105.
42. Zuo X, Song S, Zhang J, Pan D, Wang L, and Fan C “A target-responsive electrochemical aptamer switch (TREAS) for reagentless detection of nanomolar ATP.” JACS, 2007, 129, 1042–1043.
43. Rowe AA, Chuh KN, Lubin AA, Miller EA, Cook B, Hollis D and Plaxco KW, “Electrochemical biosensors employing an internal electrode attachment site achieve reversible, high gain detection of specific nucleic acid sequences.” Anal. Chem, 2011, 83, 9462–9466 [PubMed: 21975121]
44. Chamorro-Garcia A, Ortega G, Mariottini D, Green J, Ricci F, and Plaxco KW “Switching the aptamer attachment geometry can dramatically alter the signalling and performance of electrochemical aptamer-based sensors.” Chemical Communications, 2021, 57, 11693–11696. [PubMed: 34673866]
45. Farjami E, Campos R, and Ferapontova EE “Effect of the DNA end of tethering to electrodes on electron transfer in methylene blue-labeled DNA duplexes.” Langmuir, 2012, 28, 16218–16226. [PubMed: 23106377]
46. Mayer MD, and Lai RY “Effects of redox label location on the performance of an electrochemical aptamer-based tumor necrosis factor-alpha sensor.” Talanta, 2018, 189, 585–591. [PubMed: 30086964]
47. Bakhshandeh F, Zheng H, Barra NG, Sadeghzadeh S, Ausri I, Sen P, Keyvani F, Rahman F, Quadrilatero J, Liu J, Schertzer JD, Soleymani L, and Poudineh M, “Wearable aptalyzer integrates microneedle and electrochemical sensing for in vivo monitoring of glucose and lactate in live animals.” Adv Mater., 2024, e2313743. [PubMed: 38752744]
48. Kang D, Ricci F, White RJ, and Plaxco KW “Survey of redox-active moieties for application in multiplexed electrochemical biosensors.” Anal. Chem, 2016, 88, 10452–10458. [PubMed: 27659949]
49. Leung KK, Downs AM, Ortega G, Kurnik M, and Plaxco KW “Elucidating the mechanisms underlying the signal drift of electrochemical aptamer-based sensors in whole blood.” ACS sensors, 2021, 6, 3340–3347. [PubMed: 34491055]
50. Li S, Ferrer-Ruiz A, Dai J, Ramos-Soriano J, Du X, Zhu M, Zhang W, Wang Y, Herranz MÁ, Jing L, Zhang Z, Li H, Xia F, and Martín N “A pH-independent electrochemical aptamer-based biosensor supports quantitative, real-time measurement in vivo.” Chemical science, 2022, 13, 8813–8820. [PubMed: 35975161]
51. Pellitero MA, Kundu N, Sczepanski J, and Arroyo-Currás N “Os(II/III) complex supports pH-insensitive electrochemical DNA-based sensing with superior operational stability than the benchmark methylene blue reporter.” The Analyst, 2023, 148, 806–813. [PubMed: 36632808]
52. Shaver A, Curtis SD, and Arroyo-Currás N, “Alkanethiol monolayer end groups affect the long-term operational stability and signaling of electrochemical aptamer-based sensors in biological fluids.” ACS App. Mat. Interf, 2020, 12, 11214–11223
53. Ramos NC, Medlin JW, and Holewinski A “Electrochemical stability of thiolate self-assembled monolayers on Au, Pt, and Cu.” ACS Applied Materials and Interfaces, 2023, 15, 14470–14480. [PubMed: 36898023]
54. Watkins Z, Karajic A, Young T, White R, and Heikenfeld J “Week-long operation of electrochemical aptamer sensors: New insights into self-assembled monolayer degradation mechanisms and solutions for stability in serum at body temperature.” ACS Sensors, 2023, 8, 1119–1131. [PubMed: 36884003]

55. Li H, Dauphin-Ducharme P, Arroyo-Currás N, Tran CH, Vieira PA, Li S, Shin C, Somerson J, Kippin TE, and Plaxco KW “A biomimetic phosphatidylcholine-terminated monolayer greatly improves the in vivo performance of electrochemical aptamer-based sensors.” Angewandte Chemie, 2017, 56, 7492–7495. [PubMed: 28371090]
56. Kesler V, Fu K, Chen Y, Park CH, Eisenstein M, Murmann B, and Soh HT, “Tailoring electrode surface charge to achieve discrimination and quantification of chemically similar small molecules with electrochemical aptamers.” Adv Funct Mater, 2023, 33, 2208534 [PubMed: 36819738]
57. Bakestani RM, Wu Y, Glahn-Martinez B, Kippin TE, Plaxco KW, and Kolkman RW, “Carboxylate-terminated electrode surfaces improve the performance of electrochemical aptamer-based sensors.” ACS Sensors, 2025, 17, 8706–8714
58. d’Astous ÉV, and Dauphin-Ducharme P, “Whole blood multiplex measurements using electrochemical aptamer-based biosensors.” Chem Commun, 2024, 60, 6419–6422.
59. Shaver A, Mallires K, Harris J, Kavner J, Wang B, Gottlieb R, Lión-Villar J, Herranz MÁ, Martín N, and Arroyo-Currás N, “Survey of conductive polymers for the fabrication of conformation switching nucleic acid-based electrochemical biosensors.” ACS Appl Polym Mater., 2024, 6, 3572. [PubMed: 38544969]
60. Olivan LA, Hand K, and White RJ “Utilization of spontaneous alkyne-gold self-assembly chemistry as an alternative method for fabricating electrochemical aptamer-based sensors.” Langmuir, 2024, 40, 12117–12123. [PubMed: 38826127]
61. Leung KK, Gerson J, Emmons N, Heemstra JM, Kippin TE, and Plaxco K, “The use of xenonucleic acids significantly reduces the in vivo drift of electrochemical aptamer-based sensors.” Angewandte Chemie, 2024, e202316678. [PubMed: 38500260]
62. Luo S, Wu Q, Wang L, Qu H and Zheng L, “Direct detection of doxorubicin in whole blood using a hydrogel-protected electrochemical aptamer-based biosensor.” Available at SSRN: https://ssrn.com/abstract=4829481
63. Santos-Cancel M, and White RJ “Collagen membranes with ribonuclease inhibitors for long-term stability of electrochemical aptamer-based sensors employing RNA.” Anal. Chem, 2017, 89, 5598–5604. [PubMed: 28440619]
64. Li S, Dai J, Zhu M, Arroyo-Currás N, Li H, Wang Y, Wang Q, Lou X, Kippin TE, Wang S, Plaxco KW, Li H, and Xia F “Implantable hydrogel-protective DNA aptamer-based sensor supports accurate, continuous electrochemical analysis of drugs at multiple sites in living rats.” ACS Nano, 2023, 17, 18525–18538. [PubMed: 37703911]
65. Anosova I, Kowal AE, Dunn MR, Chaput JC, Van Horn WD, Egli M, “The structural diversity of artificial genetic polymers.” Nucleic Acids Research, 2016, 44, 1007–1021. [PubMed: 26673703]
66. Taylor AI, and Holliger P, “Selecting fully-modified XNA aptamers using synthetic genetics.” Curr Protoc Chem Biol, 2018, 10, e44. [PubMed: 29927117]
67. Rangel AE, Chen Z, Ayele TM, and Heemstra JM, “In vitro selection of an XNA aptamer capable of small-molecule recognition.” Nuc. Acids Res, 2018, 46, 8057–8068.
68. Lozoya-Colinas A, Yu Y, and Chaput JC, “Functionally enhanced XNA aptamers discovered by parallelized library screening.” JACS, 2023, 145, 25789–25796.
69. Arroyo-Currás N, Scida K, Ploense KL, Kippin TE, and Plaxco KW, “High surface area electrodes generated via electrochemical roughening improve the signaling of electrochemical aptamer-based biosensors.” Anal. Chem, 2017, 89, 12185–12191. [PubMed: 29076341]
70. Li S, Lin L, Chang X, Si Z, Plaxco KW, Khine M, Li H, and Xia F “A wrinkled structure of gold film greatly improves the signaling of electrochemical aptamer-based biosensors.” RSC Advances, 2021, 11, 671–677. [PubMed: 35423693]
71. Downs AM, Gerson J, Hossain MN, Ploense K, Pham M, Kraatz HB, Kippin T, and Plaxco KW “Nanoporous gold for the miniaturization of in vivo electrochemical aptamer-based sensors.” ACS Sensors, 2021, 6, 2299–2306. [PubMed: 34038076]
72. White RJ, Phares N, Lubin AA, Xiao Y, and Plaxco KW, “Optimization of electrochemical aptamer-based sensors via optimization of probe packing density and surface chemistry.” Langmuir, 2008, 24, 10513–10518. [PubMed: 18690727]

73. Wu Y, Shi J, Kippin T, and Plaxco KW “Codeposition enhances the performance of and simplifies the fabrication of electrochemical aptamer-based sensors.”, Langmuir, 2024, 40, 8703–8710. [PubMed: 38616608]
74. Liu Y, Canoura J, Alkhamis O, and Xiao Y “Immobilization strategies for enhancing sensitivity of electrochemical aptamer-based sensors.” ACS Applied Materials & Interfaces, 2021, 13, 9491–9499. [PubMed: 33448791]
75. Liu B, and Liu J “Freezing-driven DNA adsorption on gold nanoparticles: Tolerating extremely low salt concentration but requiring high DNA concentration.” Langmuir, 2019, 35, 6476–6482. [PubMed: 31008607]
76. Li Z, Lv Y, Duan X, Liu B, and Zhao Y “Highly uniform DNA monolayers generated by freezing-directed assembly on gold surfaces enable robust electrochemical sensing in whole blood.” Angewandte Chemie, 2023, 62, e202312975. [PubMed: 37726209]
77. Steichen M and Buess-Herman C, “Electrochemical detection of the immobilization and hybridization of unlabeled linear and hairpin DNA on gold.” Electrochem., 2005, 416–420
78. Keighley SD, Li P, Estrela P, Migliorato P, “Optimization of DNA immobilization on gold electrodes for label-free detection by electrochemical impedance spectroscopy.” Biosens Bioelectron., 2008, 23, 1291–1297. [PubMed: 18178423]
79. Henry OY, Perez JG, Sanchez JL, O’Sullivan CK, “Electrochemcial characterisation and hybridisation efficiency of co-assembled monolayers of PEGylated ssDNA and mercaptohexanol on planar gold electrodes.” Biosens Bioelectron., 2010, 25, 978–983. [PubMed: 19800782]
80. Fan C, Plaxco KW, and Heeger AJ *“Electrochemical* interrogation of conformational changes as a reagentless method for the sequence-specific detection of DNA.” Proceedings of the National Academy of Sciences, 2003, 100, 9134–9137.
81. Xiao Y, Piorek BD, Plaxco KW, and Heeger AJ “A reagentless signal-on architecture for electronic, aptamer-based sensors via target-induced strand displacement.” JACS, 2005, 127, 17990–17991.
82. White RJ, and Plaxco KW “Exploiting binding-induced changes in probe flexibility for the optimization of electrochemical biosensors.” Anal. Chem, 2010, 82, 73–76. [PubMed: 20000457]
83. Verrinder E, Leung KK, Erdal MK, Sepunaru L, and Plaxco KW “Comparison of voltammetric methods used in the interrogation of electrochemical aptamer-based sensors.” Sensors and Diagnostics, 2024, 3, 95–103.
84. Dauphin-Ducharme P, and Plaxco KW, “Maximizing the signal gain of electrochemical-DNA sensors.” Anal. Chem, 2016, 88, 11654–11662. [PubMed: 27805364]
85. Ferguson BS, Hoggarth DA, Maliniak D, Ploense K, White RJ, Woodward N, Hsieh K, Bonham AJ, Eisenstein M, Kippin TE, Plaxco KW, and Soh HT “Real-time, aptamer-based tracking of circulating therapeutic agents in living animals.*”* Science Translational Medicine, 2013, 5, 213ra165.
86. Verrinder E, Gerson H, Leung KK, Kippin TE, and Plaxco KW, “Dual-frequency, ratiometric approaches to EAB sensor interrogation support the calibration-free measurement of specific molecules in vivo.” ACS Sensors, 2024, 9, 3205–3211 [PubMed: 38775190]
87. Santos-Cancel M, Lazenby RA, and White RJ, “Rapid two-millisecond interrogation of electrochemical, aptamer-based sensor response using intermittent pulse amperometry.” ACS Sensors, 2018, 3, 1203–1209. [PubMed: 29762016]
88. Downs AM, Gerson J, Ploense KL, Plaxco KW, and Dauphin-Ducharme P “Subsecond-resolved molecular measurements using electrochemical phase interrogation of aptamer-based sensors.” Anal. Chem, 2020, 92, 14063–14068. [PubMed: 32959647]

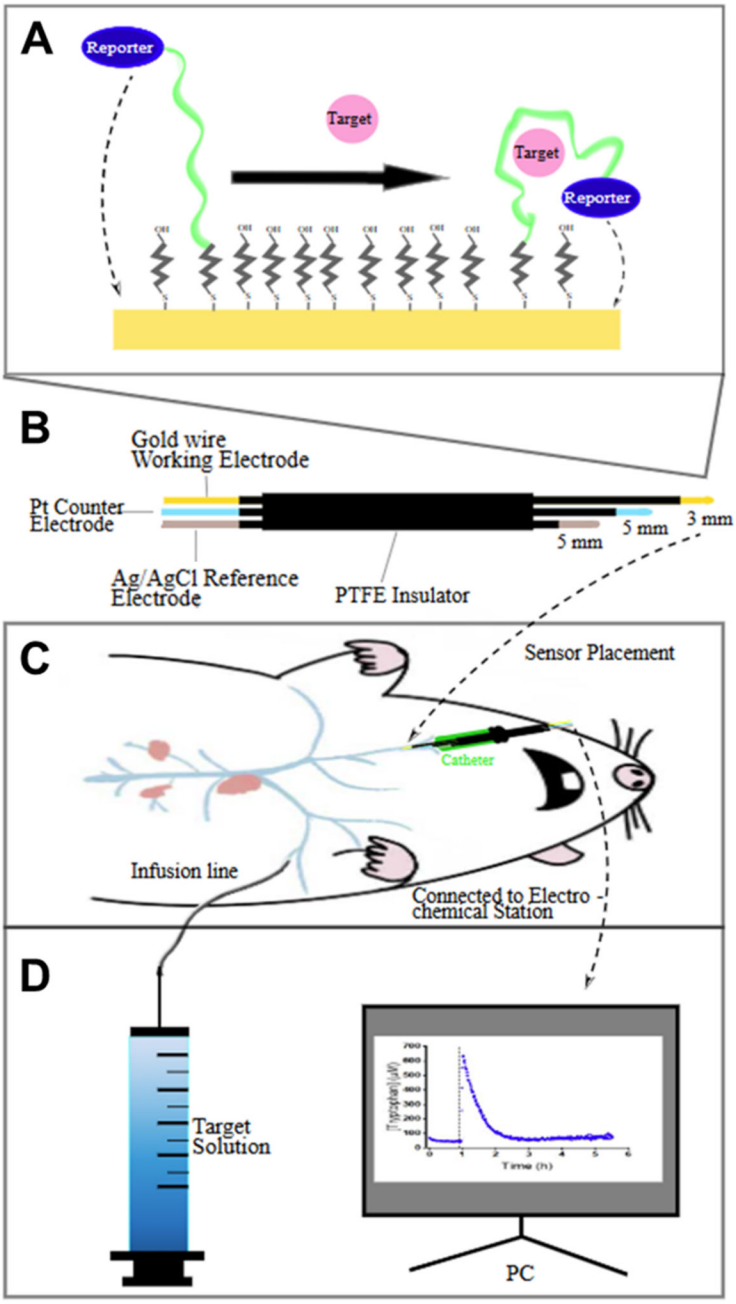

Figure 1.

(A, B) Electrochemical, aptamer-based sensors are comprised of a redox-reporter-modified, electrode-bound aptamer. The binding of the target molecule to this receptor induces a conformational change that, in turn, reduces the efficiency with which the redox reporter approaches the electrode to transfer electrons. The resulting change in electron transfer kinetics is easily measured using a variety of electrochemical methods. (C) The biomimetic nature of this conformation-linked signaling ensures that EAB sensors perform well even when deployed in situ in the body[27]. (D) We regularly use intravenous EAB sensors, for example, to monitor plasma drug and metabolite kinetics in the rat[5–9].

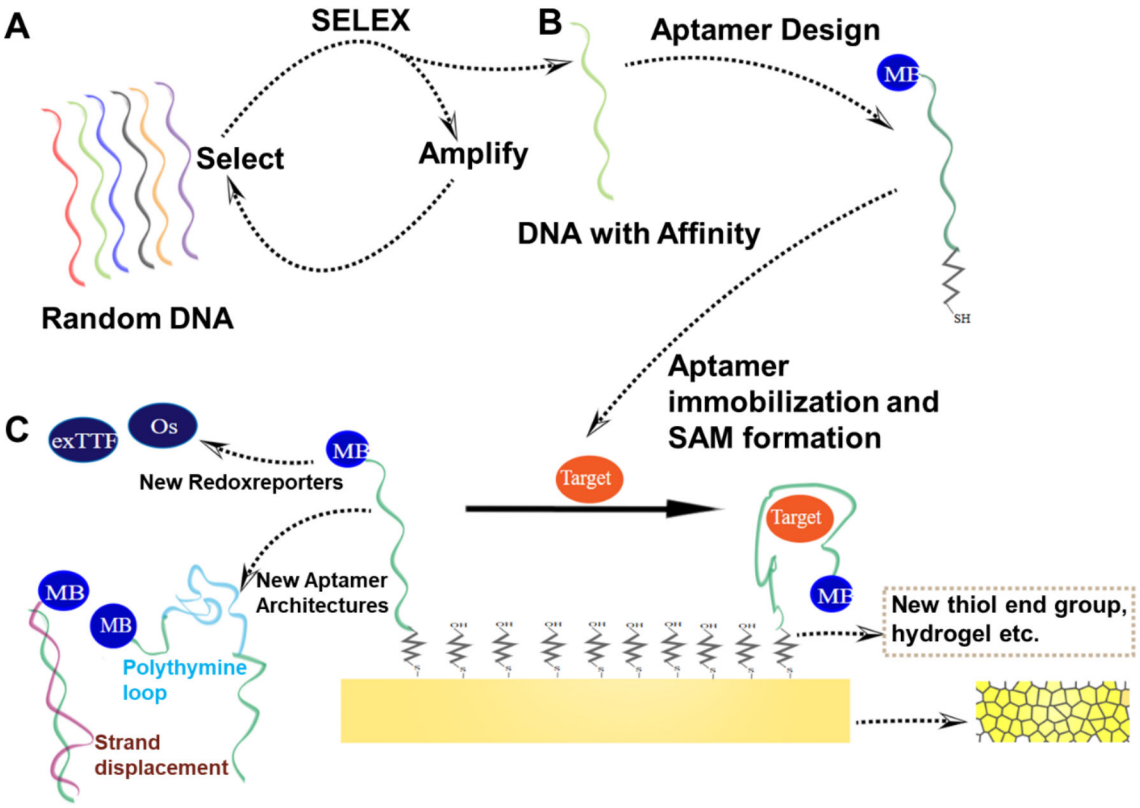

Figure 2.

(A) Aptamers are produced via an in vitro selection approach termed SELEX (systematic evolution of ligands by exponential enrichment)[31–32]. (B) To incorporate them into EAB sensors, they often must be modified such that they undergo a binding-induced conformational change[10]. (C) The aptamer is then further modified by the addition of a redox reporter (typically methylene blue -MB) and an alkane thiol, with the latter serving to anchor it to a gold electrode. Known and potential methods of improving EAB sensor performance include altering the mechanism underlying the binding-induced conformational change, the use of new redox reporters, altering the conditions employed during aptamer deposition, changing the chemistry of the electrode surface, and changing the structural morphology of the electrode.

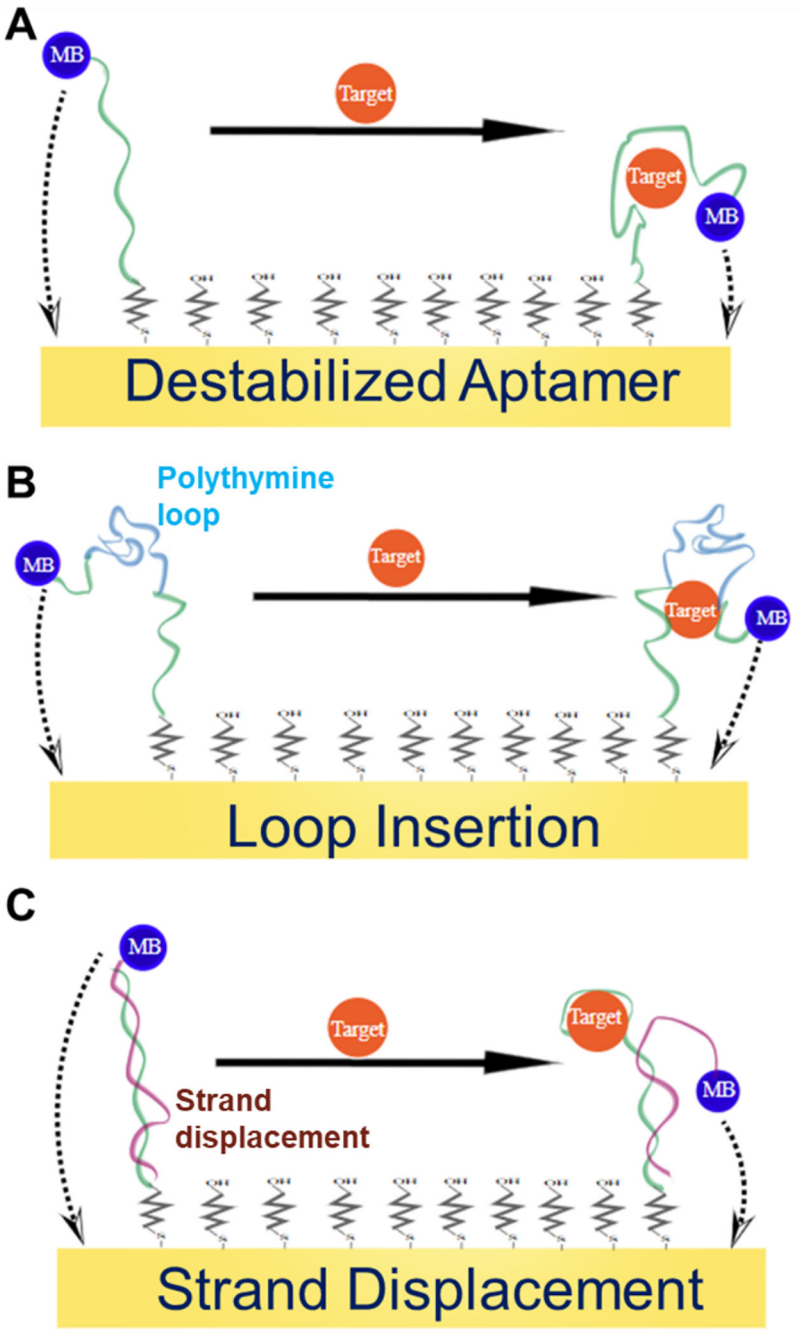

Figure 3.

Aptamers have been re-engineered to undergo a binding-induced conformational change via: (A) destabilization (using truncation or other mutations), (B) the introduction of a long, unstructured loop, or (C) the introduction of a complementary oligonucleotide strand.

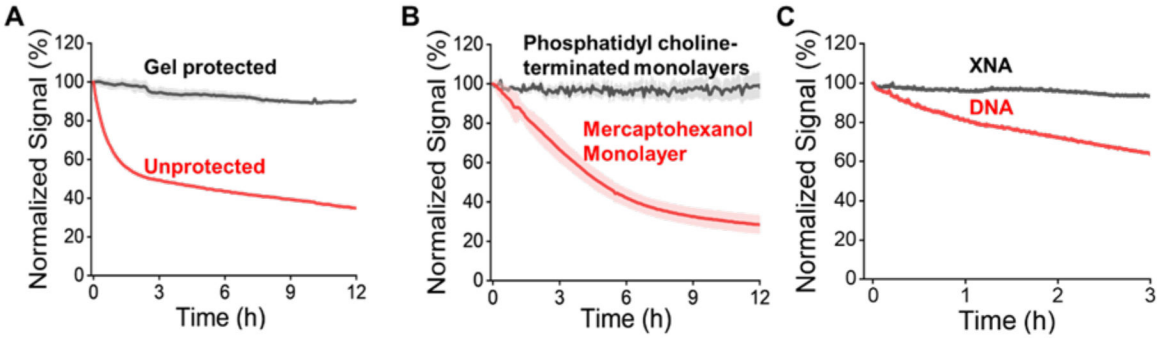

Figure 4.

Three methods of reducing the drift seen when EAB sensors are employed in complex biological matrices: (A) protection using a hydrogel that greatly reduces the speed with which macromolecules diffuse to the sensor surface[55], (B) the use of fouling-resistant phosphatidyl choline-terminated monolayers[64], and (C) the use of DNA molecules with nuclease-resistant, non-natural “xenonucleic acid” (shown is 2’-methoxyRNA versus DNA). The data in panels A and B were collected in vitro in 37°C whole blood, and in panel C in vivo in the rat jugular. Panel A adapted with permission from ref[64]. Copyright 2023 American Chemical Society. Panel B adapted with permission from ref[55]. Copyright 2017 Angewandte Chemie. Panel C adapted with permission from ref[61]. Copyright 2024 Angewandte Chemie.

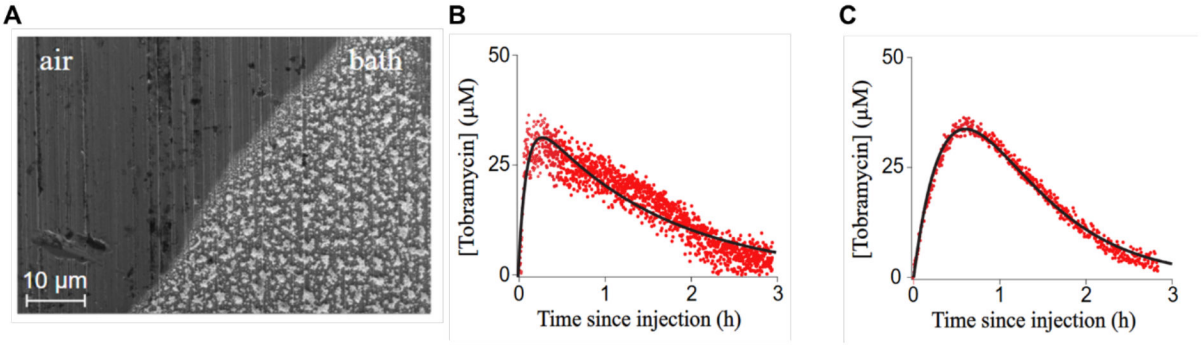

Figure 5.

By increasing the microscopic, active surface area of gold wire electrodes, electrochemical roughening increases the signal-to-noise ratios of EAB sensors of a given macroscopic size. (A) A scanning-electron micrographs taken at the location of the air–liquid interface illustrates the morphological effects of this "electroroughening"[71]. A comparison of intravenous tobramycin measurements performed in the rat jugular using (B) a smooth electrode or (C) an electroroughened electrode illustrates the resulting improvement in signal-to-noise ratios[71]. Figures adapted with permission from ref[71]. Copyright 2021 American Chemical Society.

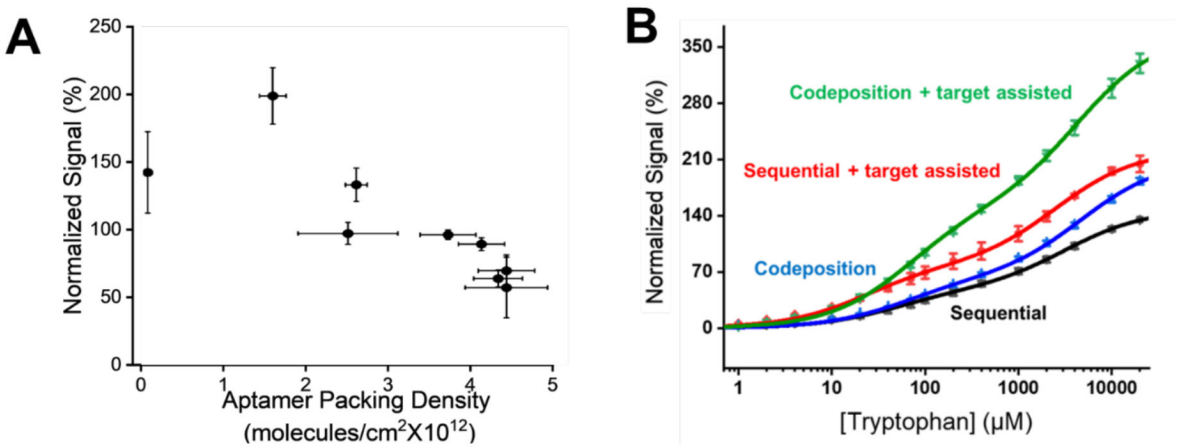

Figure 6.

(**A**) The density with which the target-binding aptamers are packed onto the surface of an EAB sensor affects its gain. The gain of a sensor against cocaine, for example, is highest at intermediate packing densities[72]. (**B**) Gain is also a function of the fabrication approach. The gain of a tryptophan-detecting sensor increases, for example, when it is fabricated either in the presence of the target (target assisted), or when the thiol-modified DNA and the alkane thiol diluent are simultaneously co-deposited rather than sequentially deposited, with the improved gain arising from the two effects being additive[73]. Panel A adapted with permission from ref[72]. Copyright 2008 American Chemical Society. Panel B adapted with permission from ref[73]. Copyright 2024 American Chemical Society.

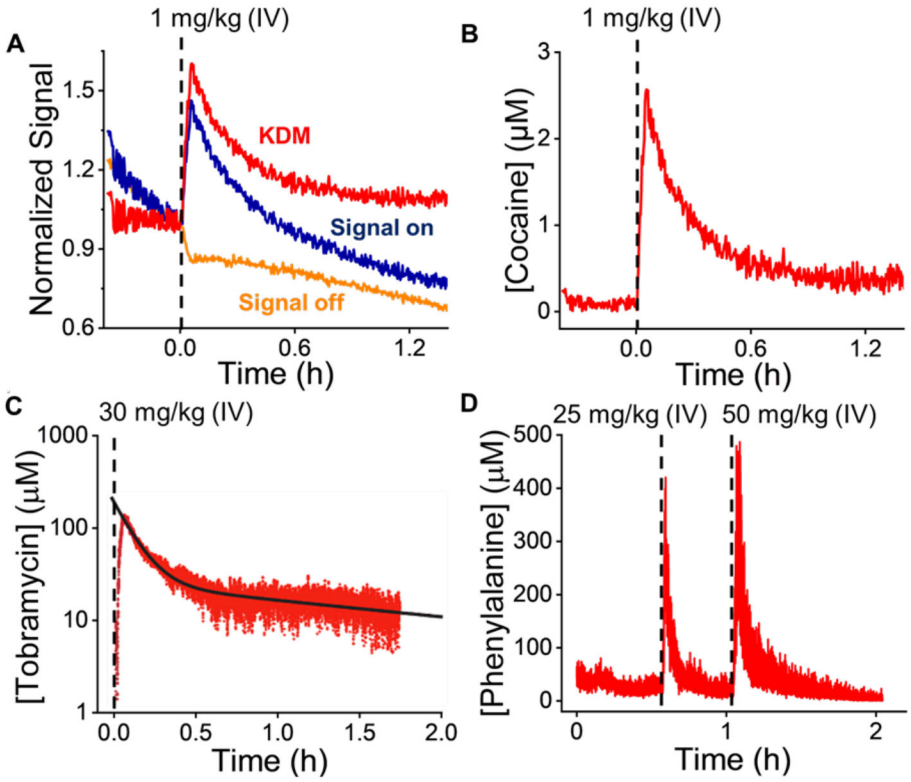

Figure 7.

A range of distinct electrochemical techniques have been used to interrogate in vivo EAB sensors. **(A)** Most in vivo examples have used square wave voltammetry drift corrected using kinetic differential measurements (KDM), an approach that employs measurements collected at a pair of square-wave frequencies that drift in concert but respond differentially to the presence of target[29,85]. Shown are "signal-on" (200 Hz), "signal-off" (20 Hz), and corrected KDM signals obtained from a cocaine-detecting sensor in the rat jugular[21]. **(B)** Using this approach, the corresponding plasma cocaine concentrations can be obtained. Given the time required to collect the pair of voltammograms, this approach typically achieves a time resolution of 10 to 20 s. **(C)** In contrast, chronoamperometry is both intrinsically drift free and able to achieve time resolution of a few hundred milliseconds. Shown here, for example, are 300-ms resolved plasma tobramycin measurements performed in the rat jugular[27]. **(D)** Fourier-transform electrochemical impedance spectroscopy is also intrinsically drift free and achieves 1 to 2 s resolution. Shown here, for example, is 1.8-s resolved plasma phenylalanine in the rat jugular[34]. Panels A and B adapted with permission from ref[21]. Copyright 2024 American Chemical Society. Panel C adapted with permission from ref[27]. Copyright 2018 American Chemical Society. Panel D adapted with permission from ref[34]. Copyright 2023 American Chemical Society.